Effect of EZH2 regulation of the JAK2/STAT3 signaling pathway on proliferation and apoptosis in non-small cell lung cancer cells

SHUANG WU[1] and WEI ZHANG[2]

[1]Department of Cardiothoracic Surgery, Yantaishan Hospital, Yantai, Shandong 264100, P.R. China;
[2]Department of Thoracic Surgery, Yantai Yuhuangding Hospital, Yantai, Shandong 264000, P.R. China

Received December 24, 2025; Accepted August 10, 2026

DOI: 10.3892/or.2026.9190

Abstract. Enhancer of zeste homolog 2 (EZH2) is frequently overexpressed in non-small cell lung cancer (NSCLC) and is associated with aggressive tumor behavior and poor patient prognosis. However, the molecular mechanisms through which EZH2 drives NSCLC progression, particularly its interplay with major oncogenic signaling cascades, remain incompletely defined. EZH2 expression was analyzed using publicly available databases. Functional perturbations were achieved via short hairpin RNA (shRNA)-mediated knockdown in NCI-H1299 and A549 NSCLC cell lines. Cell proliferation, migration, invasion, apoptosis, and colony formation were assessed using Cell Counting Kit-8, Transwell, flow cytometry and colony formation assays, respectively. Involvement of the JAK2/STAT3 pathway was examined by western blotting and rescue experiments using a JAK2 agonist. *In vivo* validation was conducted using a xenograft mouse model. EZH2 was markedly upregulated in NSCLC tissues. Its silencing markedly suppressed cell proliferation, impaired migratory and invasive capacities, induced apoptosis, and curtailed tumor growth *in vivo*. Mechanistically, EZH2 silencing attenuated the phosphorylation of both JAK2 and STAT3. Crucially, the anti-tumor effects of EZH2 knockdown were effectively reversed by JAK2 agonism, positioning EZH2 upstream of the JAK2/STAT3 axis. The present study demonstrated that EZH2 promotes NSCLC progression through activation of the JAK2/STAT3 signaling pathway, identifying the EZH2-JAK2/STAT3 axis as a potential therapeutic vulnerability in this malignancy.

Introduction

Lung cancer remains the leading cause of cancer-related mortality worldwide. In 2022, ~2.5 million new cases were diagnosed, accounting for 12.4% of all cancer diagnoses, with an estimated 1.8 million deaths representing 18.7% of global cancer mortality (1). Non-small cell lung cancer (NSCLC) constitutes ~85% of all lung cancer cases. Over the past decade, treatment paradigms for NSCLC have transitioned from conventional cytotoxic chemotherapy toward biomarker-driven precision medicine, substantially improving patient outcomes and quality of life (2,3). Following the landmark discovery linking epidermal growth factor receptor (EGFR) mutations to gefitinib efficacy, inhibitors targeting actionable drivers, including EGFR, anaplastic lymphoma kinase, ROS proto-oncogene 1, B-Raf proto-oncogene, rearranged during transfection, neurotrophic tyrosine receptor kinase, mesenchymal-epithelial transition factor and kirsten rat sarcoma viral oncogene, have been integrated into clinical practice, conferring marked survival advantages (3-5).

Nevertheless, precision therapy in NSCLC confronts persistent challenges. First, only ~25% of patients harbor currently targetable driver mutations (6); Second, median progression-free survival on targeted agents frequently remains below 20 months, constrained by acquired resistance mechanisms such as secondary mutations, bypass pathway activation, and histologic transformation (7); Third, immune checkpoint inhibitors targeting programmed cell death protein-1/programmed death-ligand 1(PD-L1) demonstrate efficacy predominantly in patients with high PD-L1 expression, yet primary resistance occurs in over 40% of these cases (8). These limitations underscore the urgent need to explore novel therapeutic strategies targeting core oncogenic signaling pathways.

The JAK2/STAT3 signaling pathway plays a pivotal role in tumorigenesis and cancer progression across multiple malignancies, regulating crucial processes including cell proliferation, apoptosis evasion, and immune modulation (9,10). Constitutive JAK2/STAT3 activation upregulates anti-apoptotic proteins and immunosuppressive factors, thereby facilitating tumor survival and immune escape (11-13).

Enhancer of Zeste Homolog 2 (EZH2), the catalytic subunit of Polycomb Repressive Complex 2 (PRC2), is a key epigenetic regulator frequently overexpressed in various cancers. In NSCLC, EZH2 expression is markedly elevated (~3.2-fold higher than in adjacent normal tissues (14,15) and contributes to tumor growth, invasion and metastasis through diverse mechanisms (16). Notably, emerging evidence implicates

Correspondence to: Professor Wei Zhang, Department of Thoracic Surgery, Yantai Yuhuangding Hospital, 20 Yuhuangding East Road 264000, Yantai, Shandong 264000 P.R. China
E-mail: ytyhdyyxwkzw@sina.com

Key words: non-small cell lung cancer, enhancer of zeste homolog 2, JAK2/STAT3, proliferation, apoptosis

crosstalk between EZH2 and JAK2/STAT3 signaling in several cancer types (17). In bladder cancer, pharmacological EZH2 inhibition suppresses tumor growth and metastasis via downregulation of the JAK2/STAT3 pathway (17). In multiple myeloma, EZH2 promotes disease progression by activating STAT3 signaling (18). In melanoma, EZH2 co-operates with STAT3 to regulate the expression of the autophagy-related gene Atg7, shaping the tumor immune microenvironment (19). In glioma, EZH2 modulates STAT3 expression and activity, influencing downstream inflammasome activation (20).

Despite these advances, the functional relationship between EZH2 and JAK2/STAT3 signaling in NSCLC remains incompletely understood. Given the established oncogenic roles of both pathways and their documented interplay in other malignancies, it was hypothesized that EZH2 promotes NSCLC progression through activation of the JAK2/STAT3 cascade. Targeting this axis may therefore represent a promising strategy to overcome treatment resistance and mitigate immune suppression in NSCLC.

Materials and methods

Reagents and antibodies. AG490, a JAK2 inhibitor, was obtained from MedChemExpress and coumermycin A1, a JAK2 agonist, was purchased from Promega Corporation. The following cell lines were obtained from Shanghai Fuheng Biotechnology: BEAS-2B (FH0319), HCC827 (FH0048), NCI-H1650 (FH0047), NCI-H1299 (FH0908) and A549 (FH0045). Cells were maintained in RPMI 1640 (BasalMedia; cat. no. L110KJ) supplemented with 10% fetal bovine serum (FBS; Vazyme Biotech Co., Ltd.; cat. no. 7E830L4) and 1% penicillin/streptomycin (P/S, Biosharp Life Sciences; cat. no. BL505A). Antibodies against β-actin (cat. no. LF212S), JAK2 (cat. no. R013499), STAT3 (cat. no. P012881), phosphorylated (p)-STAT3 (cat. no. R013862) and all secondary antibodies were purchased from Epizyme Biotech. Anti-p-JAK2 (cat. no. AF3024) was obtained from Affinity Biosciences and anti-EZH2 (cat. no. 21800-1-AP) was from Proteintech Group, Inc. Radio- immunoprecipitation assay (RIPA) lysis buffer and bicinchoninic acid (BCA) protein assay kit were procured from Beyotime Biotechnology. Reverse transcription-quantitative (RT-q) PCR reagents were sourced from Takara Bio, Inc. The FITC Annexin V Apoptosis Detection Kit was acquired from BD Biosciences. The experimental workflow is summarized in Fig. S1.

Dry lab section

Bioinformatics analyses (in silico procedures in dry lab section). EZH2 expression in lung adenocarcinoma (LUAD) tissues and adjacent normal tissues was analyzed using the GEPIA database (http://gepia.cancer-pku.cn/index.html) (21).

Wet lab Section

Cell culture. A total of four NSCLC cell lines, HCC827, NCI-H1650, NCI-H1299 and A549, were initially screened for EZH2 expression. Based on the results, NCI-H1299 and A549 cells were selected for subsequent EZH2 knockdown experiments.

To validate the role of EZH2 in JAK2/STAT3 signaling, cells were divided into the following groups: Control, sh-EZH2, JAK2 inhibitor and sh-EZH2+JAK2 agonist. Subsequent pathway analyses were conducted across these groups. For the JAK2 inhibitor group, cells were treated with 25 μmol/l AG490. For the sh-EZH2+JAK2 agonist group, EZH2-knockdown cells were treated with 10 μmol/l coumermycin A1 (CA1) (22).

Transfection. shRNA sequences targeting EZH2 and a non-targeting control were designed and synthesized by GeneChem Co., Ltd. (Shanghai, China). The sequences were as follows: shNC: 5'-TTCTCCGAACGTGTCACGT-3'; sh-EZH2 #1: 5'-GCTAGGTTAATTGGGACCA-3'; sh-EZH2 #2: 5'-CCAACACAAGTCATCCCATTA-3'. Using the second-generation lentiviral packaging system, lentiviral packaging was performed by GeneChem Co., Ltd., which used 293T cells as the packaging cell line. The shRNA-containing pLKO.1-TRC vector was co-transfected with the packaging plasmid psPAX2 and envelope plasmid pMD2.G at a ratio of 4:3:1, with a total of 10 μg of lentiviral plasmid per transfection, using Lipofectamine® 2000 (Thermo Fisher Scientific, Inc.). Cells were incubated at 37˚C for 48-72 h. Viral supernatant was harvested, filtered through 0.22 μm pore-size filters (Millipore), and used for transduction.

For transduction, NCI-H1299 and A549 cells were seeded into 6-well plates ($2x10^5$ cells/well) at 70-90% confluence. The harvested lentivirus was diluted in complete medium to a titer of $1x10^8$ TU/ml, and 60 μl/well (MOI=30) was added to the cells. Polybrene (5 μg/ml; MilliporeSigma) was added to enhance transduction efficiency. Cells were incubated at 37˚C for 24 h, after which the medium was replaced with fresh complete medium. After an additional 48 h of culture, stable transfectants were selected using 2.5 μg/ml puromycin for 7 days.

Cell derived xenograft. Female BALB/c nude mice (4-6 weeks old, n=6 per group) were used for the experiments (23,24), purchased from Jinan Pengyue Laboratory Animal Breeding Co., Ltd. All mice were housed under specific pathogen-free (SPF) conditions with free access to food and water and were monitored daily for general health and behavior. The housing environment was maintained at a temperature of 22±2˚C with a relative humidity of 50±10%, and a 12-h light/dark cycle. All efforts were made to minimize suffering and distress throughout the experiment. A total of 12 mice were used in the present study. Female mice were selected following the practice of previous xenograft studies (23,24). The skin on the lumbar and abdominal regions was disinfected using povidone-iodine. Mice were divided into two groups: The negative control group (shNC) received a subcutaneous injection of 0.1 ml of control A549 cell suspension ($5x10^6$ cells), and the experimental (shEZH2) group received the same volume of EZH2-knockdown A549 cell suspension (25). Humane endpoints were defined as tumor volume exceeding 1,500 mm^3, or tumor ulceration, necrosis, or infection accompanied by severe clinical signs of distress (such as ruffled fur, reduced appetite, or decreased activity). Any mouse meeting these criteria was immediately sacrificed prior to the scheduled endpoint. The experiment was terminated on day 28 post-inoculation. No mice were found dead or required early sacrifice prior to the scheduled endpoint. On day 28 post-inoculation, all mice were sacrificed by CO_2 inhalation at a flow rate of 30% chamber volume per min until respiration ceased followed by cervical dislocation. Mortality

was confirmed by the absence of spontaneous respiration, loss of corneal reflex, and lack of response to toe pinch. Tumor tissues were then excised for subsequent experiments.

Cell Counting Kit-8 (CCK-8). Cell viability was assessed using the CCK-8 kit (Dojindo Laboratories, Inc.). Cells (3,000-5,000 per well) were seeded in 96-well plates. Subsequently, 10 μl of CCK-8 solution was added to each well and incubated at 37˚C for 3 h. Absorbance was measured at 450 nm.

RT-qPCR. Total RNA was extracted from NCI-H1299 and A549 cells using RNAiso Plus (Takara Bio, Inc.) and reverse-transcribed into cDNA using PrimeScript™ RT Master Mix (Takara Bio, Inc.), both according to the manufacturers' protocols. qPCR was performed on a CFX-96 system (Bio-Rad Laboratories, Inc.) using TB Green Premix Ex Taq (Takara Bio, Inc.) under the following conditions: 95˚C for 10 sec, 55˚C for 15 sec and 72˚C for 20 sec. Cycle threshold values were normalized to β-actin. Primer sequences were: EZH2 (F) GTACACGGGGATAGAGAATGTGG, (R) GGTGGGCGG CTTTCTTTATCA; β-actin (F) AACACCCCAGCCATGTAC GTT, (R) CCATCTCTTGCTCGAAGTCCA. Relative expression was calculated using the $2^{-\Delta\Delta Cq}$ method (26).

Colony formation assay. Cells were seeded at 500 cells per well in a 6-well plate and culture continued for 14 days (27). The medium was changed every three days and the cells observed. Once colonies (defined as a cluster of >50 cells) had formed, they were washed once with PBS. Then 4% paraformaldehyde (1 ml) was added to each well for 30 min at room temperature. The cells were washed once with PBS. Crystal violet staining solution (1 ml) was added to each well and the cells stained for 10-20 min at room temperature. After washing, the cells were air-dried and images captured using a digital camera.

Cell migration and invasion assays. Migration and invasion were evaluated using Transwell chambers without or with Matrigel coating, respectively. For the invasion assay, Transwell chambers were precoated with Matrigel at 37˚C for 1 h. Following sh-EZH2 transfection, cells were serum-starved for 12 h. Complete medium (600 μl) containing 10% FBS was added to the lower chamber, and 200 μl of cell suspension ($5x10^5$ cells/ml in serum-free medium) was seeded into the upper chamber. After 24 h, cells on the lower surface were fixed with 4% paraformaldehyde at room temperature for 20 min, stained with crystal violet at room temperature for 15 min, and images captured under a light microscope at x200 magnification. Images of five randomly selected fields per chamber were captured (28).

Apoptosis assay. Cells were suspended in 1X binding buffer at $1x10^5$ cells/ml, stained with Annexin V-FITC and PI at room temperature in the dark for 20 min, and analyzed by flow cytometry (Accuri™ C6; BD Biosciences) using FlowJo software (v10.8.1; BD Biosciences). The apoptotic rate was calculated as the percentage of early apoptotic cells (Annexin V-$FITC^+/PI^-$) plus late apoptotic cells (Annexin V-$FITC^+/PI^+$). TUNEL staining was performed on tumor tissue using an TMR (red) tunel cell apoptosis detection kit (Wuhan Servicebio Technology Co., Ltd.) according to the manufacturer's protocol. Following dewaxing and rehydrating, 4-μm thick paraffin sections were incubated with proteinase K at 37˚C for 20 min. Following completion of the reaction, the sections were washed with PBS and excess liquid was gently flicked off. Membrane-breaching solution was added and the sections were incubated at room temperature for 20 min. After washing with PBS, the sections were incubated with buffer for 10 min. Subsequently, TDT enzyme, dUTP, and buffer in a 2:5:50 ratio were mixed and the sections were incubated at 37˚C for 1 h. Nuclei were counterstained with DAPI at room temperature for 10 min, and sections were visualized under a fluorescence microscope (Leica Microsystems GmbH).

Western blotting. Total proteins were extracted from NCI-H1299 and A549 cells using RIPA lysate (Beyotime Biotechnology). After measuring the protein concentration by BCA (Beyotime Biotechnology), the protein samples (20 μg per lane) were separated on 10% gels using sodium dodecyl sulfate-polyacrylamide gel electrophoresis (SDS-PAGE) and transferred onto the polyvinylidene difluoride (PVDF) membranes blocked with 5% non-fat milk at room temperature for 1 h and incubated with the primary antibodies [EZH2 (1:5,000; cat. no. 21800-1-AP; Proteintech Group, Inc.), JAK2 (1:500; cat. no. R013499; Epizyme Biotech), STAT3 (1:1,000; cat. no. P012881; Epizyme Biotech), p-JAK2 (1:1,000; cat. no. AF3024; Proteintech Group, Inc.), p-STAT3 (1:500; cat. no. R013862; Epizyme Biotech) and β-actin (1:5,000; cat. no. LF212S; Epizyme Biotech)] at 4˚C overnight. Membranes were then incubated with HRP-conjugated secondary antibodies (1:10,000; cat. no. LF102; Epizyme Biotech) for 2 h at room temperature. Signals were detected using enhanced chemiluminescence (ECL) substrate kit (Vazyme Biotech Co., Ltd.), and band intensities were quantified with ImageJ (version 1.54p; National Institutes of Health) (29).

Hematoxylin and eosin (H&E) staining. A tissue sample ~1 cm in length was excised from the tumor tissue, fixed in 4% formaldehyde solution at room temperature for 24 h, followed by dehydration (70, 80, 90, 95 and 100% ethanol), clearing in xylene and embedding in paraffin wax. The paraffin-embedded tissues were cut into 4-μm-thick sections, dewaxed and rehydrated. Sections were stained with hematoxylin at room temperature for 5 min, followed by eosin for 2 min, and then dehydrated, cleared and mounted. Images were captured under a light microscope (Zeiss AG).

Immunohistochemistry (IHC) staining. After dewaxing and rehydrating, 4-μm thick paraffin sections were subjected to heat-induced antigen retrieval in citrate buffer at 95˚C for 15 min. Sections were incubated with 3% H_2O_2 at room temperature for 30 min to block endogenous peroxidase activity. After blocking with 3% bovine serum albumin (BSA; Wuhan Servicebio Technology Co., Ltd.) at room temperature for 30 min, sections were incubated with Ki-67 primary antibody (1:800; cat. no. GB111499; Wuhan Servicebio Technology Co., Ltd.) overnight at 4˚C, followed by HRP-conjugated goat anti-rabbit secondary antibody (1:500; cat. no. GB23303; Wuhan Servicebio Technology Co., Ltd.) for 60 min at 37˚C. Staining was developed with DAB (cat. no. G1212-200T; Wuhan Servicebio Technology Co., Ltd.), counterstained with hematoxylin for 3 min at room temperature, dehydrated, cleared, and mounted. Images were captured using a light microscope (Zeiss AG).

Statistical analysis. Data were presented as mean ± standard deviation (SD). Statistical analyses were performed using GraphPad Prism (v 8; Dotmatics). Differences between groups

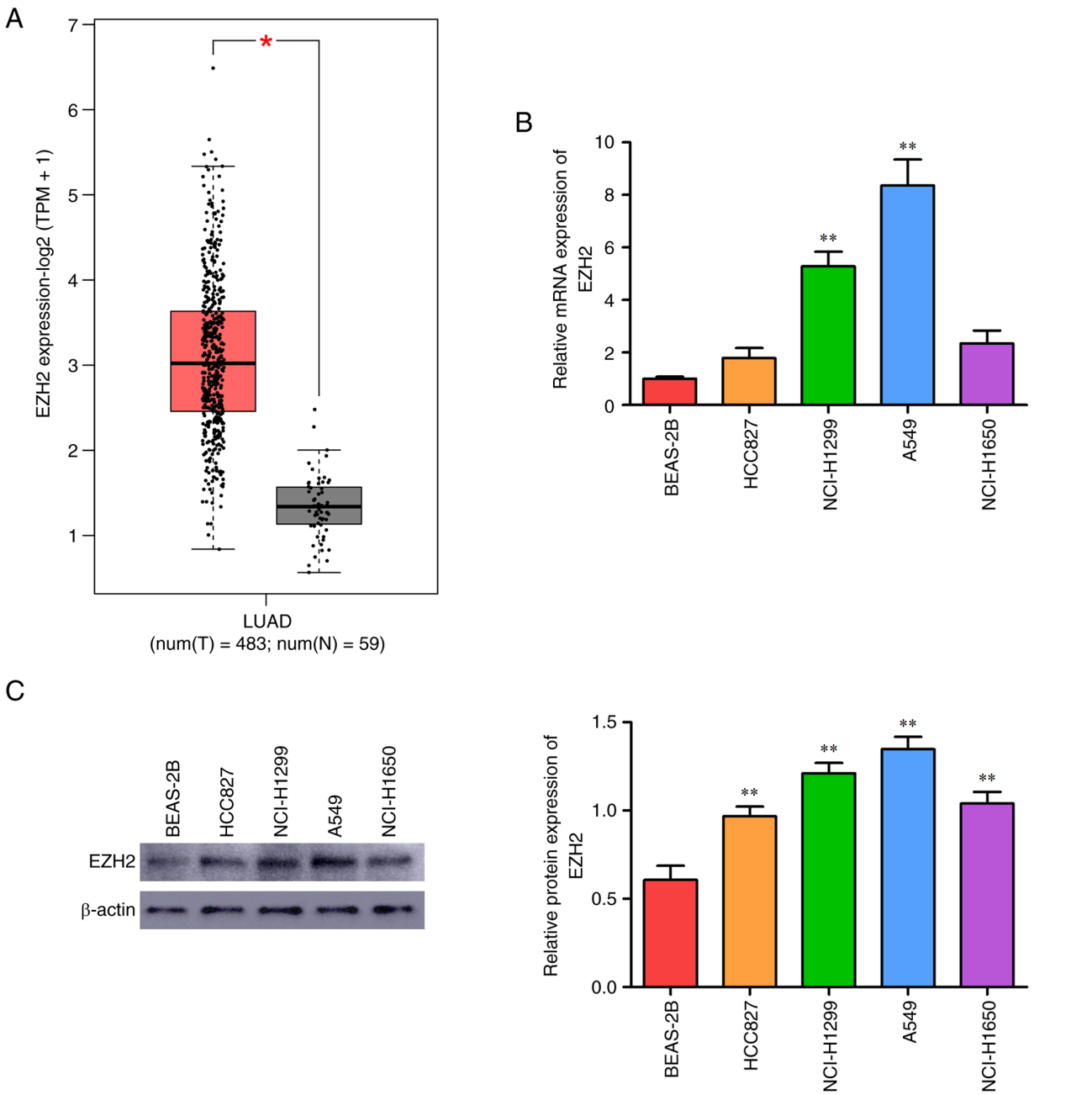

Figure 1. EZH2 expression is enhanced in LUAD. (A) EZH2 expression in LUAD tissues and normal tissues. EZH2 level in lung cancer-associated cells HCC827, NCI-H1299, A549, NCI-H1650 and BEAS-2B was determined by (B) western blotting and (C) RT-qPCR. *P<0.05, **P<0.01 vs. BEAS-2B. EZH2, enhancer of zeste homolog 2; LUAD, lung adenocarcinoma; RT-qPCR, reverse transcription-quantitative PCR.

were assessed using Student's t-test or one-way ANOVA with Tukey's post hoc test. P<0.05 was considered to indicate a statistically significant difference.

Results

EZH2 expression is upregulated in LUAD. To investigate the potential oncogenic role of EZH2, the present study analyzed its expression pattern using the GEPIA database. EZH2 was markedly upregulated in LUAD tissues compared to adjacent normal tissues (Fig. 1A).

EZH2 is highly expressed in lung cancer cell lines. EZH2 protein and mRNA levels were assessed in the normal bronchial epithelial cell line BEAS-2B and four NSCLC cell lines (HCC827, NCI-H1650, NCI-H1299, and A549) by RT-qPCR (Fig. 1B) and western blotting (Fig. 1C). EZH2 expression was markedly higher in all cancer cell lines relative to BEAS-2B. Notably, NCI-H1299 and A549 cells exhibited the highest EZH2 levels and were therefore chosen for functional studies.

EZH2 knockdown suppresses proliferation and induces apoptosis via JAK2/STAT3 pathway. Stable EZH2-knockdown models were established in NCI-H1299 and A549 cells using two independent shRNAs, with knockdown efficiency confirmed by RT-qPCR (Fig. 2A). CCK-8 assays demonstrated that EZH2 silencing markedly reduced cell

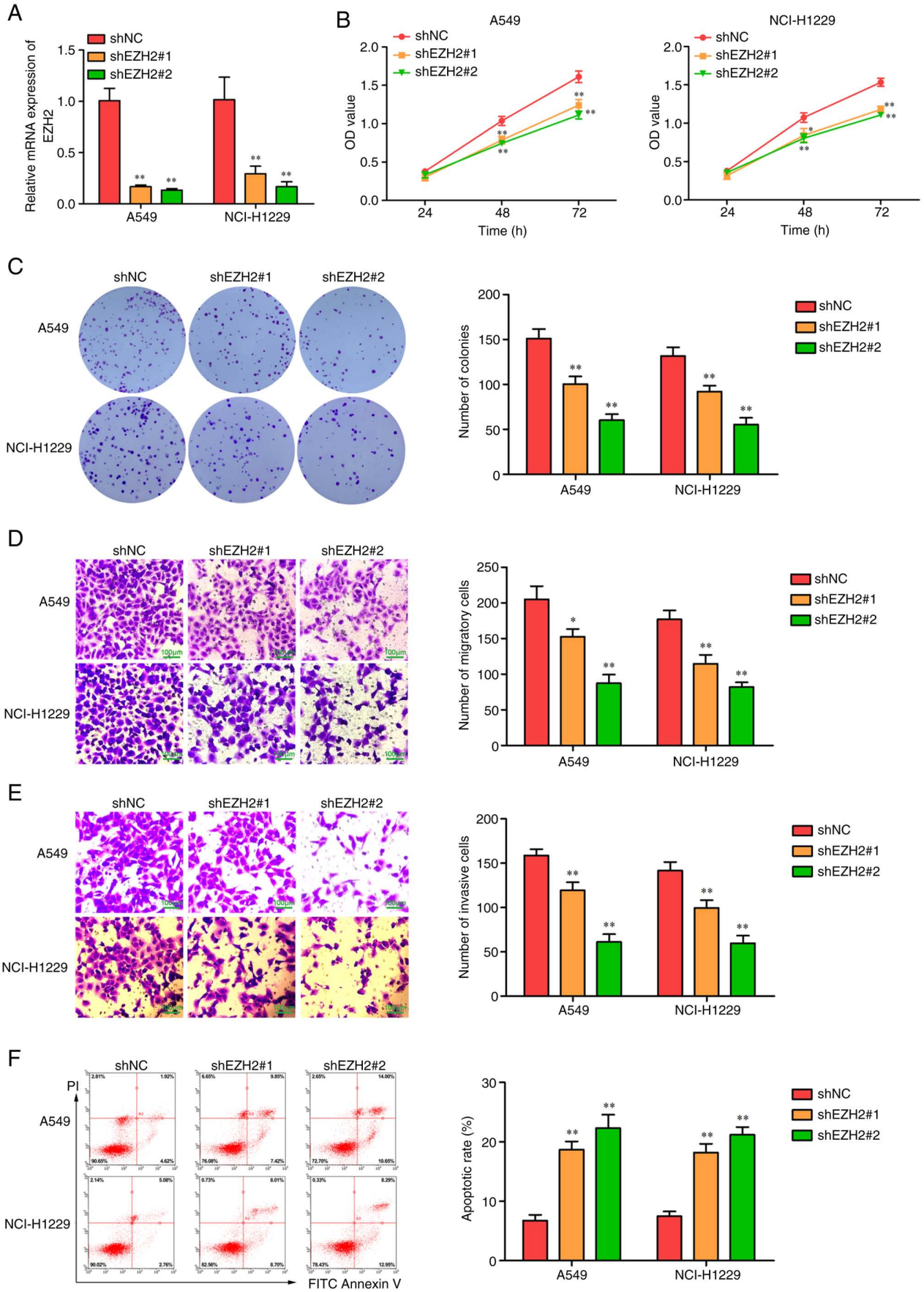

Figure 2. Knockdown of EZH2 inhibits the proliferation and migration of A549 and NCI-H1299 cells while promoting apoptosis. (A) RT-qPCR analysis of EZH2 knockdown efficiency. (B) CCK-8 assay of cell viability after transfection. (C) Colony formation assay of clonogenic proliferation. (D) Transwell assay of cell migration. Scale bar, 100 μm; magnification, x200. (E) Transwell assay of cell Invasion. Scale bar, 100 μm; magnification, x200. (F) Flow cytometric analysis of apoptosis. *P<0.05, **P<0.01 vs. shNC. EZH2, enhancer of zeste homolog 2; RT-qPCR, reverse transcription-quantitative PCR; sh, short hairpin; NC, negative control.

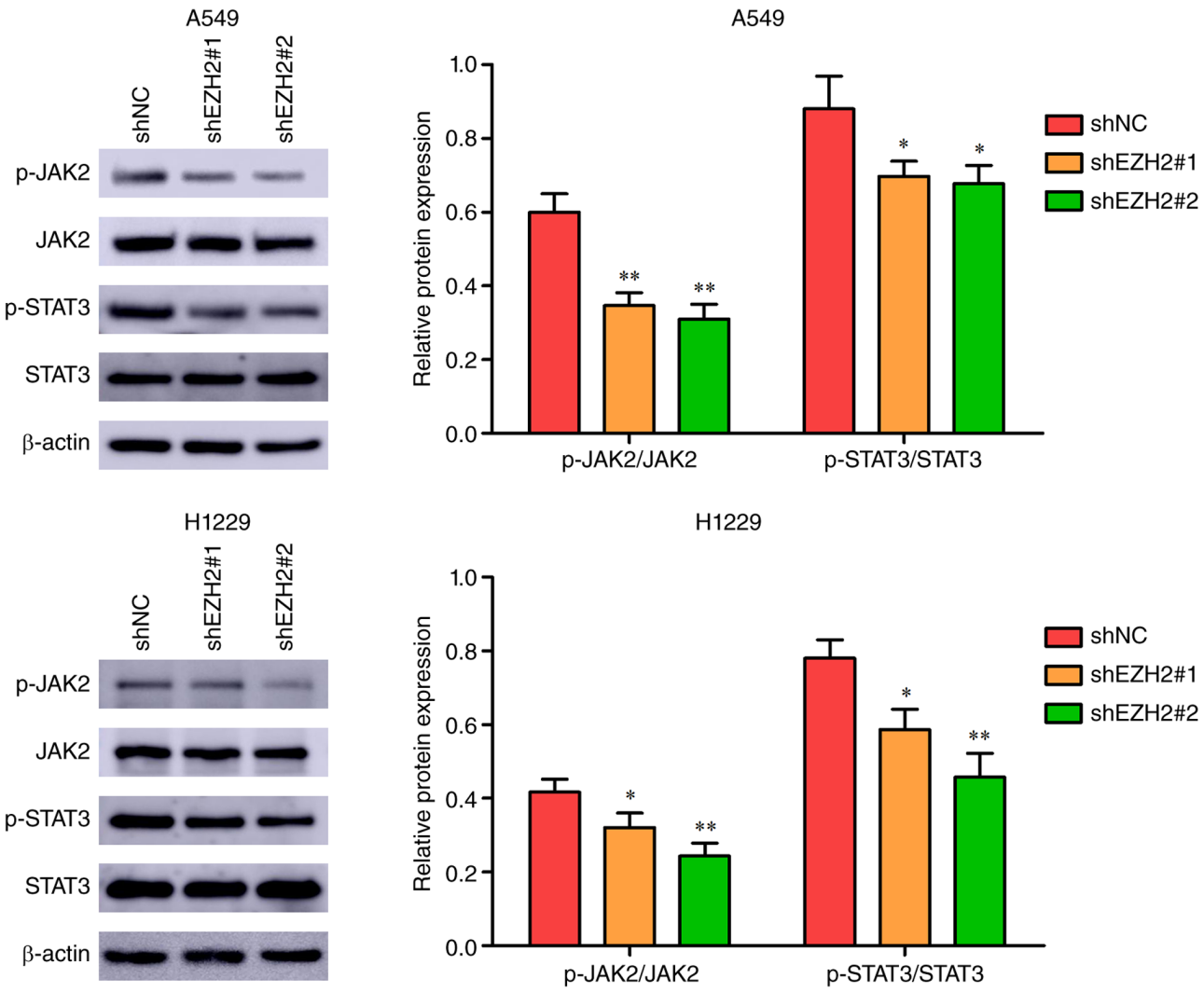

Figure 3. Knockdown of EZH2 reduced JAK2/STAT3 phosphorylation in A549 and NCI-H1299 cells. Representative western blots and quantitative analysis of EZH2, p-JAK2, JAK2, p-STAT3, STAT3, and β-actin in EZH2-knockdown A549 and NCI-H1299 cells. *P<0.05, **P<0.01 vs. shNC. EZH2, enhancer of zeste homolog 2; p-, phosphorylated; sh, short hairpin; NC, negative control.

viability (Fig. 2B). Moreover, migration, invasion, and colony formation were markedly impaired (Fig. 2C-E). Flow cytometry revealed a significant increase in apoptosis upon EZH2 knockdown (Fig. 2F).

To explore the underlying molecular mechanism, the present study examined the effect of EZH2 knockdown on the JAK2/STAT3 signaling pathway. Mechanistically, western blot analysis showed that EZH2 knockdown substantially reduced the phosphorylation levels of JAK2 and STAT3 (Fig. 3), suggesting that EZH2 promotes tumor survival and proliferation primarily through activation of this signaling cascade.

Rescue experiments confirm EZH2 acts upstream of JAK2/STAT3. To define the functional hierarchy between EZH2 and JAK2/STAT3, rescue experiments were performed using CA1 (10 μmol/l), a JAK2 agonist, and AG490 (25 μmol/l), a JAK2 inhibitor (22). JAK2 activation restored cell proliferation in EZH2-knockdown A549 and NCI-H1299 cells (Fig. 4A). Likewise, JAK2 activation effectively rescued the impaired migration, invasion, and colony formation, and attenuated the apoptosis induced by EZH2 silencing (Fig. 4B-E). Western blotting confirmed that JAK2 inhibition reduced p-JAK2 and p-STAT3 without affecting EZH2 expression (Fig. 5), whereas JAK2 activation in EZH2-knockdown cells restored both p-JAK2 and p-STAT3 levels.

EZH2 silencing suppresses tumor growth in vivo via inhibiting JAK2/STAT3. Since A549 cells exhibited more pronounced phenotypic changes upon EZH2 knockdown compared to NCI-H1299 cells *in vitro*, A549 cells were selected for the xenograft model. Control or EZH2-knockdown A549 cells were inoculated into nude mice. Tumors in the EZH2-knockdown group (shEZH2) exhibited markedly slower growth, reduced volume, and decreased weight compared to controls (Fig. 6A-C). H&E staining revealed a looser histological architecture in shEZH2 group tumors (Fig. 6D). Immunohistochemical staining for Ki-67 demonstrated markedly reduced proliferation in the shEZH2 group (Fig. 6E), while TUNEL staining indicated a significant increase in apoptosis (Fig. 6F). Western blot analysis of tumor confirmed reduced

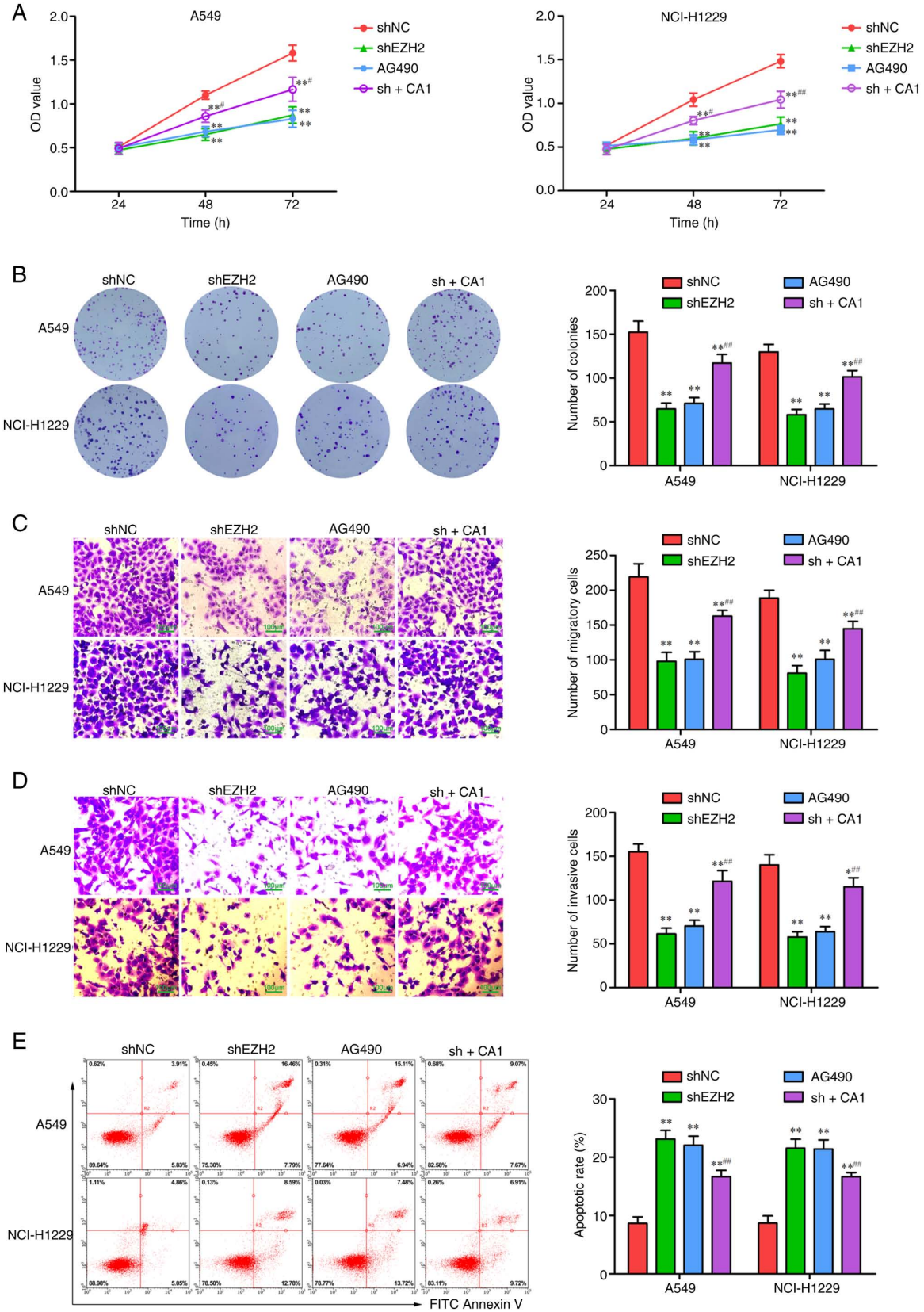

Figure 4. Reversal by a JAK2 agonist of the phenotypic effects of EZH2 knockdown, including inhibited proliferation/migration and promoted apoptosis. (A) CCK-8 assay of cell viability after transfection. (B) Colony formation assay of clonogenic proliferation. (C) Transwell assay of cell migration. Scale bar, 100 μm; magnification, x200. (D) Transwell assay of cell invasion. Scale bar, 100 μm; magnification, x200. (E) Flow cytometric analysis of apoptosis. *P<0.05, **P<0.01 vs. shNC; $^{\#}$P<0.05, $^{\#\#}$P<0.01 vs. shEZH2. EZH2, enhancer of zeste homolog 2; p-, phosphorylated; sh, short hairpin; NC, negative control; CA1, JAK2 agonist.

JAK2 and STAT3 phosphorylation, consistent with *in vitro* observations (Fig. 6G). These *in vivo* results corroborate that EZH2 facilitates tumor growth and survival primarily through JAK2/STAT3 pathway activation.

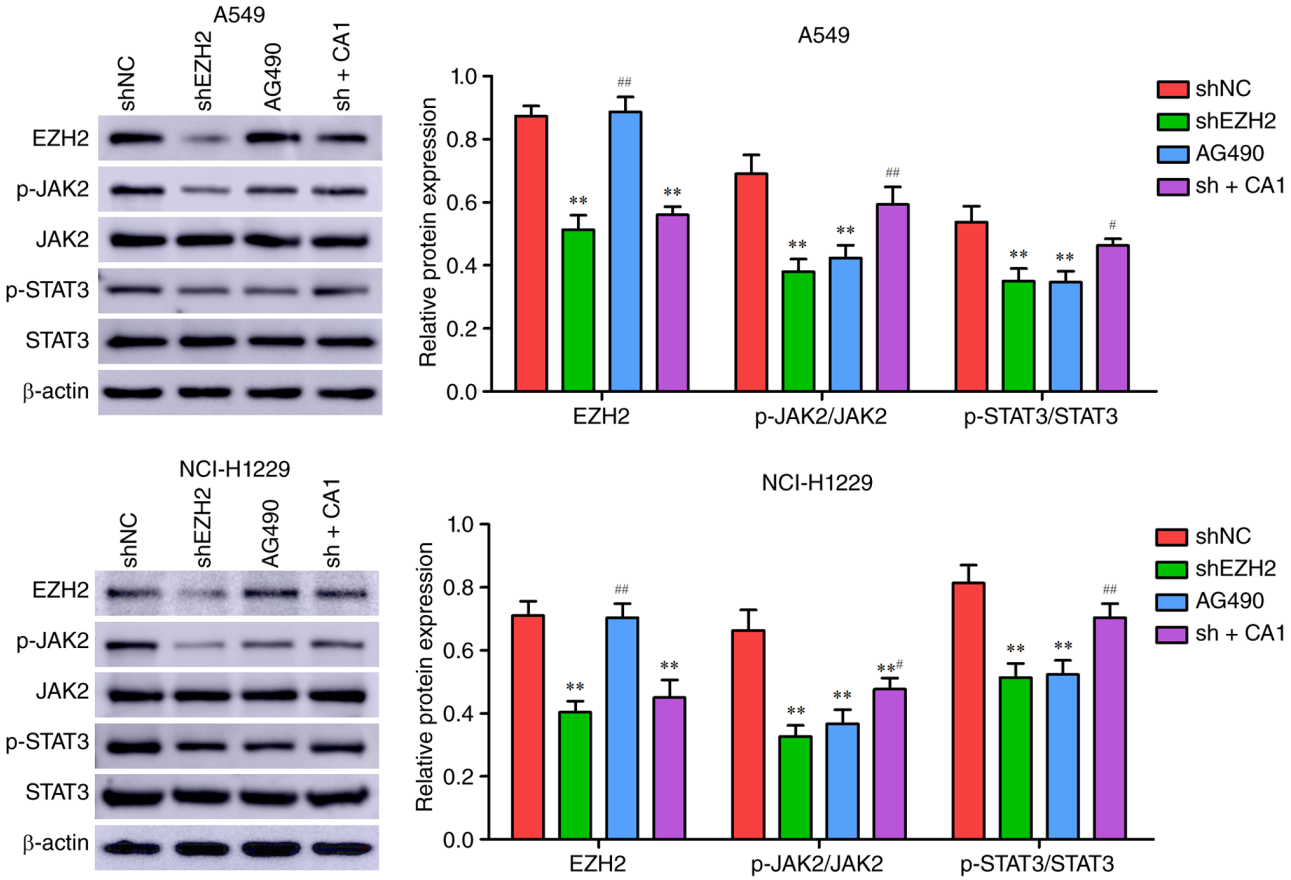

Figure 5. The inhibition of the JAK2/STAT3 pathway resulting from EZH2 knockdown was reversed by a JAK2 agonist. Representative western blots and quantitative analyses of p-JAK2, JAK2, p-STAT3, STAT3, and β-actin were performed in A549 and NCI-H1299 cells treated with shNC, shEZH2, AG490, and shEZH2 + CA1. **P<0.01 vs. shNC; $^{\#}$P<0.05, $^{\#\#}$P<0.01 vs. shEZH2. EZH2, enhancer of zeste homolog 2; AG490, JAK2 inhibitor; CA1, JAK2 agonist; p-, phosphorylated; sh, short hairpin; NC, negative control.

Discussion

The present study systematically investigated the expression, function and molecular mechanism of EZH2 in NSCLC. The key findings demonstrated that EZH2 is markedly overexpressed in LUAD tissues and multiple NSCLC cell lines. Functional experiments, both *in vitro* and *in vivo*, confirmed that EZH2 knockdown effectively suppresses proliferation and migration while inducing apoptosis. All quantitative data were presented as mean ± SD, and the differences were statistically significant, supporting the reliability of our findings. Mechanistically, EZH2 functions as an upstream regulator of the JAK2/STAT3 signaling pathway and exerts its oncogenic effects through positive regulation of this cascade, as consistently demonstrated in both *in vitro* and *in vivo* models.

EZH2, an epigenetic regulator, is highly expressed in various malignancies, including NSCLC. Prior studies indicate that EZH2 expression is markedly higher in NSCLC tissues than in normal counterparts and its overexpression correlates with tumor invasiveness, metastasis and poor prognosis (30,31). The findings of the present study aligned with extensive existing research, further supporting the critical role of EZH2 in lung cancer progression. In addition to validating the prognostic implications, the present study demonstrated through *in vitro* models and *in vivo* xenografts that EZH2 directly governs malignant behaviors-proliferation and apoptosis-in NCI-H1299 and A549 cells, providing a strong rationale for targeting EZH2 therapeutically.

The most significant contribution of the present study was the elucidation of a functional linkage between EZH2 and JAK2/STAT3 signaling in NSCLC. Rescue experiments provided compelling evidence that the oncogenic functions of EZH2 are mediated through this pathway: JAK2 agonism effectively reversed the proliferation inhibition, apoptosis induction and reduced JAK2/STAT3 phosphorylation elicited by EZH2 knockdown. This finding unequivocally positioned EZH2 upstream of the JAK2/STAT3 pathway. Previous studies have reported similar interactions between EZH2 and JAK2/STAT3 signaling in other cancer types. In bladder cancer, pharmacological inhibition of EZH2 was shown to suppress tumor growth through downregulation of the JAK2/STAT3 pathway (32). Notably, our recent study demonstrated that norcantharidin exerts anti-tumor effects in NSCLC through downregulation of EZH2/JAK2/STAT3 signaling pathway (17). However, these studies primarily relied on pharmacological inhibitors and did not establish a clear functional hierarchy between EZH2 and the JAK2/STAT3 pathway. By contrast, the present study provided the first characterization of this regulatory relationship in NSCLC using genetic EZH2 knockdown combined with rescue experiments. Mechanistically, previous studies have demonstrated that EZH2 regulates JAK2 expression

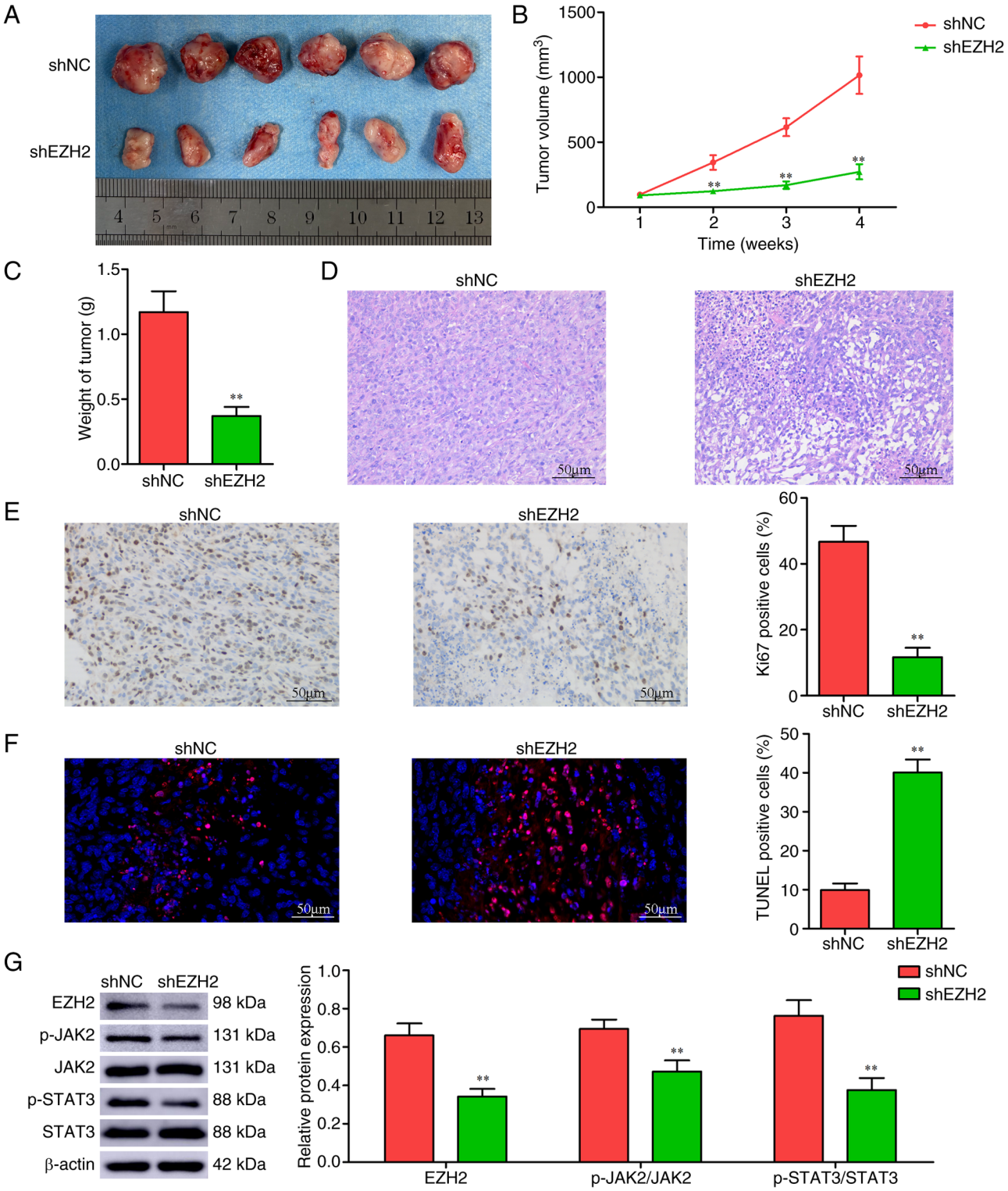

Figure 6. EZH2 silencing suppresses tumor growth *in vivo* by inhibiting JAK2/STAT3. (A) The tumor image at day 28. (B) Tumor volumes at day 7, 14, 21 and 28 were calculated. (C) Tumor weight on day 28. (D) Hematoxylin and eosin staining, (E) Ki-67 immunohistochemistry and (F) TUNEL staining of tumor tissue. (G) Representative western blot and quantitative analysis for EZH2, p-JAK2, JAK2, p-STAT3, STAT3 and β-actin. **P<0.01 vs. shNC. EZH2, enhancer of zeste homolog 2; p-, phosphorylated; sh, short hairpin; NC, negative control.

by modifying the H3K27me3 histone mark in its promoter region (33,34). However, the present study revealed that EZH2 knockdown reduced JAK2 and STAT3 phosphorylation without markedly altering their total protein levels. The precise mechanism underlying this regulation requires further investigation.

Persistent JAK2/STAT3 activation is intimately linked to tumor cell proliferation, apoptosis resistance and the establishment of an immunosuppressive microenvironment (35-37). Notably, Toll-like receptors (TLRs) play a role in modulating immune responses within the tumor microenvironment and TLR-guided therapeutic strategies have been explored as

promising approaches for cancer immunotherapy (38,39). Given that EZH2 acts upstream of JAK2/STAT3 signaling pathway and has been implicated in epigenetic regulation of immune-related genes (40), targeting EZH2 may represent a more promising strategy to suppress the abnormal activation of this pathway and reshape the immunosuppressive microenvironment at its source. Currently, several EZH2 inhibitors are under clinical investigation (41-43). Given its established role in resistance mechanisms, EZH2 inhibitors, whether used alone or in combination with JAK2 or immune checkpoint inhibitors, merit investigation as a therapeutic strategy for patients who have progressed on existing targeted or immunotherapies.

The present study has several strengths. First, the present study employed two independent shRNA sequences to knock down EZH2, minimizing off-target effects and ensuring the specificity of the observations. Second, the combination of genetic knockdown with pharmacological rescue experiments using both a JAK2 agonist and inhibitor allowed the establishment of a functional hierarchy between EZH2 and the JAK2/STAT3 pathway. Third, the consistency of the findings across *in vitro* cell models and an *in vivo* xenograft model provided robust evidence for the role of the EZH2-JAK2/STAT3 axis in NSCLC progression.

Of course, the present study had certain limitations. First, while the present study demonstrated that EZH2 acts upstream of the JAK2/STAT3 pathway, the precise molecular mechanism by which EZH2 regulates JAK2/STAT3 phosphorylation remains unclear. Additional mechanistic studies, such as ChIP-qPCR, promoter analyses, or protein interaction assays, are needed to determine whether EZH2 directly regulates JAK2 expression or affects pathway activation indirectly. Furthermore, given the classical role of EZH2 as the PRC2 catalytic subunit mediating H3K27 trimethylation, future studies using H3K27me3 analysis or pharmacological EZH2 inhibitors are required to clarify whether the observed effects rely on EZH2 methyltransferase activity, especially given recent evidence of methyltransferase-independent EZH2 functions in other types of cancer (44). Second, EZH2 overexpression rescue experiments would further strengthen the causal relationship between EZH2 and the JAK2/STAT3 pathway, which will be pursued in future studies. Third, the present study primarily focused on the NCI-H1299 and A549 cell lines; the generalizability of these findings to other NSCLC subtypes requires validation in additional models. Additionally, the use of only female mice in the present study may introduce sex-related bias. Future studies will include both male and female animals to further validate the generalizability of our findings. Finally, *in vivo* studies could be expanded, such as using conditional knockdown mouse models, to more precisely elucidate the role of EZH2 in lung cancer development.

In summary, the present study established that EZH2 drives malignant progression in NSCLC through activation of the JAK2/STAT3 signaling pathway. These findings deepen our understanding of EZH2-mediated oncogenesis and, more importantly, highlight the therapeutic potential of targeting the EZH2-JAK2/STAT3 axis to overcome drug resistance and immune suppression in NSCLC, offering new insights and experimental rationale for the development of novel combination therapeutic strategies.

Acknowledgements

Not applicable.

Funding

No funding was received.

Availability of data and materials

The data generated in the present study may be requested from the corresponding author.

Authors' contributions

SW and WZ confirm the authenticity of all the raw data. SW and WZ contributed to the study conception and design. Writing, reviewing and editing, resources, supervision and conceptualization were performed by WZ. The writing of the original draft, formal analysis, software and figure preparation (visualization) were carried out by SW, and both authors commented on previous versions of the manuscript. Both authors have read and approved the final manuscript.

Ethics approval and consent to participate

The animal experiments were performed in accordance with ARRIVE guidelines and were approved by the Ethics Committee of Yuhuangding Hospital (Shandong, China; approval no. K2025-381).

Patient consent for publication

Not applicable.

Competing interests

The authors declare that they have no competing interests.

References

1. Bray F, Laversanne M, Sung H, Ferlay J, Siegel RL, Soerjomataram I and Jemal A: Global cancer statistics 2022: GLOBOCAN estimates of incidence and mortality worldwide for 36 cancers in 185 countries. CA Cancer J Clin 74: 229-263, 2024.
2. Goldstraw P, Ball D, Jett JR, Le Chevalier T, Lim E, Nicholson AG and Shepherd FA: Non-small-cell lung cancer. Lancet 378: 1727-1740, 2011.
3. Wu YL, Tsuboi M, He J, John T, Grohe C, Majem M, Goldman JW, Laktionov K, Kim SW, Kato T, *et al*: Osimertinib in resected EGFR-Mutated non-small-cell lung cancer. N Engl J Med 383: 1711-1723, 2020.
4. Meyer ML, Fitzgerald BG, Paz-Ares L, Cappuzzo F, Jänne PA, Peters S and Hirsch FR: New promises and challenges in the treatment of advanced non-small-cell lung cancer. Lancet 404: 803-822, 2024.
5. Parvaresh H, Roozitalab G, Golandam F, Behzadi P and Jabbarzadeh Kaboli P: Unraveling the potential of ALK-Targeted therapies in non-small cell lung cancer: Comprehensive insights and future directions. Biomedicines 12: 297, 2024.
6. Gao W, Wang L, Zhao Y and Zhu L: The role of PD-L1 in EGFR-mutant non-small cell lung cancer. Discov Oncol 16: 307, 2025.
7. Wiest N, Majeed U, Seegobin K, Zhao Y, Lou Y and Manochakian R: Role of immune checkpoint inhibitor therapy in advanced EGFR-Mutant non-small cell lung cancer. Front Oncol 11: 751209, 2021.

8. Aguilar EJ, Ricciuti B, Gainor JF, Kehl KL, Kravets S, Dahlberg S, Nishino M, Sholl LM, Adeni A, Subegdjo S, *et al*: Outcomes to first-line pembrolizumab in patients with non-small-cell lung cancer and very high PD-L1 expression. Ann Oncol 30: 1653-1659, 2019.
9. Rah B, Rather RA, Bhat GR, Baba AB, Mushtaq I, Farooq M, Yousuf T, Dar SB, Parveen S, Hassan R, *et al*: JAK/STAT signaling: Molecular targets, therapeutic opportunities, and limitations of targeted inhibitions in solid malignancies. Front Pharmacol 13: 821344, 2022.
10. Thomas SJ, Snowden JA, Zeidler MP and Danson SJ: The role of JAK/STAT signalling in the pathogenesis, prognosis and treatment of solid tumours. Br J Cancer 113: 365-371, 2015.
11. Chen L, Sun R and Fang K: Erianin inhibits tumor growth by promoting ferroptosis and inhibiting invasion in hepatocellular carcinoma through the JAK2/STAT3/SLC7A11 pathway. Pathol Int 74: 119-128, 2024.
12. Li Y, Wang M, Bai J, Li X, Xiao S and Song L: Anthocyanins in black soybean coats promote apoptosis in hepatocellular carcinoma cells by regulating the JAK2/STAT3 pathway. Int J Mol Sci 26: 1070, 2025.
13. Wu L, Li J, Liu T, Li S, Feng J, Yu Q, Zhang J, Chen J, Zhou Y, Ji J, *et al*: Quercetin shows anti-tumor effect in hepatocellular carcinoma LM3 cells by abrogating JAK2/STAT3 signaling pathway. Cancer Med 8: 4806-4820, 2019.
14. Cheng Y, Song Z, Fang X and Tang Z: Polycomb repressive complex 2 and its core component EZH2: Potential targeted therapeutic strategies for head and neck squamous cell carcinoma. Clin Epigenetics 16: 54, 2024.
15. Cao W, Ribeiro Rde O, Liu D, Saintigny P, Xia R, Xue Y, Lin R, Mao L and Ren H: EZH2 promotes malignant behaviors via cell cycle dysregulation and its mRNA level associates with prognosis of patient with non-small cell lung cancer. PLoS One 7: e52984, 2012.
16. Pan YM, Wang CG, Zhu M, Xing R, Cui JT, Li WM, Yu DD, Wang SB, Zhu W, Ye YJ, *et al*: STAT3 signaling drives EZH2 transcriptional activation and mediates poor prognosis in gastric cancer. Mol Cancer 15: 79, 2016.
17. Wu S and Zhang W: Norcantharidin inhibits the EZH2-mediated JAK2/STAT3 signaling pathway to inhibit the proliferation of non-small cell lung cancer. Toxicol Appl Pharmacol 507: 117714, 2026.
18. Wang Y, Tian J, Huang D, Gao Y, Lin H, Liu L and Wang A: EZH2 promotes multiple myeloma progression via STAT3 pathway activation. Discov Med 36: 721-729, 2024.
19. Zimmerman SM, Suh E, Smith SR and Souroullas GP: Stat3-mediated Atg7 expression regulates anti-tumor immunity in mouse melanoma. Cancer Immunol Immunother 73: 218, 2024.
20. Yu D, Wang S, Wang J, Zhang K, Niu Z and Lin N: EZH2-STAT3 signaling pathway regulates GSDMD-mediated pyroptosis in glioblastoma. Cell Death Discov 10: 341, 2024.
21. Ranjbar R, Behzadi P and Mammina C: Respiratory tularemia: Francisella tularensis and microarray probe designing. Open Microbiol J 10: 176-182, 2016.
22. Xiang L, Wang Y, Liu S, Ying L, Zhang K, Liang N, Li H, Luo G and Xiao L: Quercetin attenuates KLF4-Mediated phenotypic switch of VSMCs to macrophage-like cells in atherosclerosis: A critical role for the JAK2/STAT3 pathway. Int J Mol Sci 25: 7755, 2024.
23. Jin S, Zhang D, Liao Z, Yu L, Wang Y, Jia P, Pan M, Li Y and Zhang J: TRIM46 deficiency-induced DNA damage enhances the sensitivity of cisplatin in non-small cell lung cancer by regulating the Akt signaling pathway. Oncol Rep 55: 58, 2026.
24. Zheng WW, Ding JX, Liang YX and Ye L: Hydroxypropyl-β-cyclodextrin/thymoquinone inclusion complex inhibits non-small cell lung cancer progression through NF-κB-mediated ferroptosis. Oncol Rep 54: 157, 2025.
25. Chen H, Wu X, Zhu M, Cheng Y and Feng Q: Glutamine starvation induces ferroptosis in NSCLC via AMPK/PDZD8-Mediated ferritinophagy. Nutrients 18: 1596, 2026.
26. Livak KJ and Schmittgen TD: Analysis of relative gene expression data using real-time quantitative PCR and the 2(-Delta Delta C(T)) method. Methods 25: 402-408, 2001.
27. Li JX, Tan SY, Li LQ, Zheng YH, Zhao L, Zhu HR, He HL, Zhang YY, Li RZ, Bao TY, *et al*: Tricin selectively combats KRAS-mutant non-small cell lung cancer by inhibiting the PDGF-BB-induced SRC/MAPK/AP-1/PD-L1 signaling pathway and potentiating the antitumor effect of an anti-PD-1 antibody. Front Pharmacol 16: 1594213, 2025.
28. Ma G, Feng J, Zeng J, Liao R, Zhong X, Lv Z and Chen F: β-sitosterol suppresses malignant biological behaviors and glycolysis via modulating YBX1-hnRNP K interaction in non-small cell lung cancer. Sci Rep 16: 19105, 2026.
29. Jiang P, Chen Z, Cui L, Zhang N and Gao K: ID1 in TAMs promoted the progression of non-small-cell carcinoma via increasing NF-κB/NPM1/SHP1/SHP2 signaling induced M2 polarization. Sci Rep 16: 14222, 2026.
30. Kim NY and Pyo JS: Clinicopathological significance and prognostic role of EZH2 expression in non-small cell lung cancer. Pathol Res Pract 213: 778-782, 2017.
31. Shi B, Behrens C, Vaghani V, Riquelme EM, Rodriguez-Canales J, Kadara H, Lin H, Lee J, Liu H, Wistuba I and Simon G: Oncogenic enhancer of zeste homolog 2 is an actionable target in patients with non-small cell lung cancer. Cancer Med 8: 6383-6392, 2019.
32. Chen Z, Du Y, Liu X, Chen H, Weng X, Guo J, Wang M, Wang X and Wang L: EZH2 inhibition suppresses bladder cancer cell growth and metastasis via the JAK2/STAT3 signaling pathway. Oncol Lett 18: 907-915, 2019.
33. Chandnani N, Gupta I, Thakkar V and Sarkar K: Epigenetic regulation of enhancer of zeste homolog 2 (EZH2) -Yin Yang 1 (YY1) axis in cancer. Pathol Res Pract 251: 154885, 2023.
34. Dreger H, Ludwig A, Weller A, Stangl V, Baumann G, Meiners S and Stangl K: Epigenetic regulation of cell adhesion and communication by enhancer of zeste homolog 2 in human endothelial cells. Hypertension 60: 1176-1183, 2012.
35. Johnson DE, O'Keefe RA and Grandis JR: Targeting the IL-6/JAK/STAT3 signalling axis in cancer. Nat Rev Clin Oncol 15: 234-248, 2018.
36. Li C, Song J, Guo Z, Gong Y, Zhang T, Huang J, Cheng R, Yu X, Li Y, Chen L, *et al*: EZH2 inhibitors suppress colorectal cancer by regulating macrophage polarization in the tumor microenvironment. Front Immunol 13: 857808, 2022.
37. Xue C, Yao Q, Gu X, Shi Q, Yuan X, Chu Q, Bao Z, Lu J and Li L: Evolving cognition of the JAK-STAT signaling pathway: autoimmune disorders and cancer. Signal Transduct Target Ther 8: 204, 2023.
38. Mukherjee S, Patra R, Behzadi P, Masotti A, Paolini A and Sarshar M: Toll-like receptor-guided therapeutic intervention of human cancers: Molecular and immunological perspectives. Front Immunol 14: 1244345, 2023.
39. Behzadi P, García-Perdomo HA and Karpiński TM: Toll-Like receptors: General molecular and structural biology. J Immunol Res 2021: 9914854, 2021.
40. Hamad J, Tarabain NE, Soufan F, Fayyad-Kazan M, Issa N and Fayyad-Kazan H: Beyond oncogenesis: The emerging role of EZH2 in tumor microenvironment. Crit Rev Oncol Hematol 226: 105454, 2026.
41. Italiano A, Soria JC, Toulmonde M, Michot JM, Lucchesi C, Varga A, Coindre JM, Blakemore SJ, Clawson A, Suttle B, *et al*: Tazemetostat, an EZH2 inhibitor, in relapsed or refractory B-cell non-Hodgkin lymphoma and advanced solid tumours: A first-in-human, open-label, phase 1 study. Lancet Oncol 19: 649-659, 2018.
42. Song Y, Liu Y, Li ZM, Li L, Su H, Jin Z, Zuo X, Wu J, Zhou H, Li K, *et al*: SHR2554, an EZH2 inhibitor, in relapsed or refractory mature lymphoid neoplasms: A first-in-human, dose-escalation, dose-expansion, and clinical expansion phase 1 trial. Lancet Haematol 9: e493-e503, 2022.
43. Zeng D, Liu M and Pan J: Blocking EZH2 methylation transferase activity by GSK126 decreases stem cell-like myeloma cells. Oncotarget 8: 3396-3411, 2017.
44. Kuser-Abali G, Noguchi F, Zhao P, Szeto P, Zhang Y, Huang C, Barlow CK, Pomilio G, Boudes M, Chew C, *et al*: Cytosolic EZH2-IMPDH2 complexes regulate melanoma progression and metastasis via GTP. Mol Cell 86: 2521-2538.e10, 2026.